The calculation of near and far fields for acoustic antennas consisting of piezoelectric rectangular bimorph transducers in flexural vibration

A. Petrauskas

Prof. K. Baršauskas Ultrasound Institute
Kaunas University of Technology
Studentų st. 50, LT-51368 Kaunas, Lithuania
E-mail: Algimantas.Petrauskas@ktu.lt

Abstract

In this article the calculation, along with practical examples of near and far fields of acoustic antennas are presented. Knowing the near and far fields is important because the radiation patterns and physical measurements of the antennas depend on them. These antennas designed for measurements in air consist of transducers in flexural vibration, which give the best possibility to match acoustic impedances between air and the transducer. Specific type of transducers for acoustic antennas is described along with their schematic diagrams. Optimal design of the antenna is achieved when the near and far fields of the transducer are available. The near and far fields are described by the distribution of acoustic pressure in the area around the transducer. The necessary expressions for calculating acoustic pressure are supplied. In addition, diagrams of acoustic pressure distribution in chosen planes and lines of the environment are presented. Unidirectional radiation of the evaluated transducer in flexural vibration is achieved by a relatively small increase in the physical dimensions of the antenna. Schematic diagrams of actual antennas along with their radiation patterns are presented. A method for eliminating peripheral radiation of these antennas is also described.

Keywords: Near field, far field, acoustic antenna, acoustic measurements, piezoelectric transducer, flexural vibration, acoustic impedance, radiation pattern, parallel nodal lines, distribution of acoustic pressure

Introduction

For measurements in air (gas) environment, piezoelectric ceramic transducers in flexural vibration are widely used [1-12]. By using transducers in a flexural vibration there is a best possibility to match acoustic impedances between air and the transducer, because flexural transducers are characterized by a sufficiently low acoustic impedance. It is then possible to achieve optimal transmission and reception of measurement signals to air and back to the transducer.

Flexural vibrations are generated most efficiently by using unimorph, bimorph or multimorph piezoelectric transducers [1-16].

When measuring in an air environment, unidirectional transmission and reception of signals is preferred. Additionally, the peripheral transmission-reception should be as minimal as possible, because it is disruptive and produces measurement errors. Therefore, acoustic antennas consisting of piezoelectric transducers in flexural vibration are designed with a minimal peripheral transmission-reception.

The radiation pattern, along with the shape and the size of acoustic antennas, depend on the near and far fields created by electro-acoustically active elements. The near and far fields are described by the distribution of acoustic pressure in the area around the transducer. The near and far fields depend on the shape of vibrations on the transducer‘s surface [14-28].

The radiation patterns of piezoelectric ceramic transducers were investigated in papers [29-39].

It is possible to achieve unidirectional radiation of piezoelectric transducers by using rectangular bimorph piezoelectric transducers with parallel nodal lines of vibration [12-17]. Their working surfaces must be thin-walled and rectangular.

When designing acoustic antennas, piezoelectric ceramic rectangular thin-plate transducers in cosinusoidal flexural vibration can also be used [11, 14, 16]. As will be mentioned below, the required radiation patterns for these antennas can be easily obtained.

The relatively easily manageable radiation patterns can be obtained when nodal lines of vibration on the surface of the rectangular bimorph transducer are straight and parallel to one another [11, 12, 14-17]. The radiation of these transducers in a plane perpendicular to the surface of the transducer and parallel to the nodal lines of vibrations is the same as an acoustic field generated by an oscillating piston. In a perpendicular plane, if the flexural transducer is flat and is fixed on an infinite flat baffle, this transducer reveals a primary two-leaf radiation pattern and the inclination angle α between the surface of the transducer and a plane, perpendicular to the direction of radiation.

This angle depends on the ratio of velocities of acoustic waves in the transducer and in air [14-17]:

$$\sin\alpha_{1,2} = \pm\frac{k_\delta \lambda_a}{2l}, \qquad (1)$$

where α is the angle between a normal to a flat surface and direction of radiation; λ_a is the length of acoustic wave in air; k_δ is the number of nodal lines on the surface of the transducer; l is the length of a transducer in the direction of flexural vibration.

As described in [14-16], after choosing special dimensions for piezoelectric ceramic and elastic plates, resonance flexural vibration can be excited in the elastic plate, which is fixed on a rectangular frame along the whole perimeter. The design of such transducer is presented in Fig. 1.

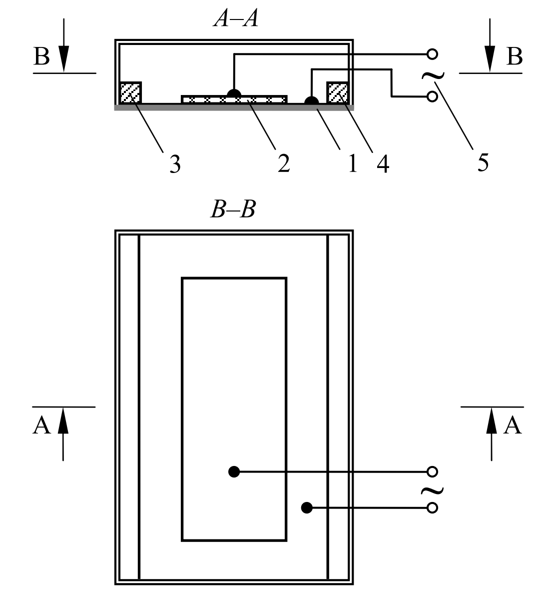

Fig.1. **Symmetric bimorph piezoelectric ceramic transducer with fixed edges: 1 – rectangular elastic plate; 2 – piezoelectric ceramic plate; 3, 4 – rectangular frame; 5 – electric excitation**

The piezoelectric ceramic transducer (Fig. 1) consists of one rectangular piezoelectric ceramic plate of normal polarization. The plate is mounted on a thin rectangular elastic plate, which is fixed on a rectangular frame along the whole perimeter. When electric pulses are applied to the electrodes of the piezoelectric ceramic plate, cosinusoidal flexural vibrations are being excited in the ceramic plate. Nodal lines of the flexural vibration are always present transversely and longitudinally on the surface of the piezoelectric ceramic plate.

In practical applications we have noticed that the third mode of cosinusoidal flexural vibration is the most interesting (Fig. 2).

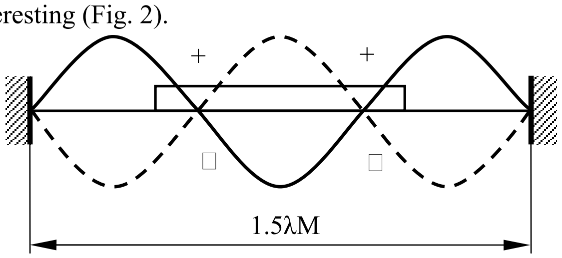

Fig.2. **The shape of the third mode of flexural vibration transversely to the surface of the transducer (Fig. 1)**

In this case, the resonance flexural vibrations are excited in the transducer, when the piezoelectric ceramic plate resonates in the second mode (two nodal lines) and the elastic plate resonates in the third mode (four nodal lines).

Theoretical analysis

Optimal design of the antenna can be achieved when the near and far fields of the transducer are available. The near and far fields are described by the distribution of acoustic pressure in the area around the transducer. When the near and far fields of the acoustic transducer are available, then by specially phasing the vibrations of the transducer and absorbing the unwanted peripheral radiation, the optimal radiation pattern of the antenna is obtained [14-17]. The following expression is used to calculate the acoustic pressure p, originating from the surface of the flat radiator, which is fixed on an infinite flat shield [39]:

$$p = \frac{j\omega\rho}{2\pi}\iint_S \dot{\xi}_0 \frac{e^{-jkr}}{r} dS, \tag{2}$$

where $\dot{\xi}_0$ is the imaginary vibration velocity on the surface of the acoustic radiator, S is the surface area of the acoustic radiator, r is the distance from the elementary surface dS of the acoustic radiator to the required point in the environment, $k = 2\pi/\lambda$ is the wave number of the flexural wave in the environment, λ is acoustic wavelength in the environment, ω is the cyclic frequency, ρ is the density of the environment, $j = \sqrt{-1}$.

The following expression is used to calculate the acoustic pressure $\dot{P}_0$, originating from the elementary surface dS of the acoustic radiator, which is fixed on an infinite flat baffle, to the required point M_0 with coordinates (x_0, y_0, z_0) (Fig. 3) in the environment [39]:

$$P_0 = -\frac{\rho\omega^2}{2\pi}\int_{-a}^{+a}\int_{-b}^{+b}\xi(x,y)\frac{e^{-jk\sqrt{(x-x_0)^2+(y-y_0)^2+z_0^2}}}{\sqrt{(x-x_0)^2+(y-y_0)^2+z_0^2}}dxdy, \tag{3}$$

where a, b are the half-width and half-length of a rectangular transducer, $\dot{\xi}(x,y)$ is the imaginary vibration velocity on the surface of the rectangular acoustic radiator.

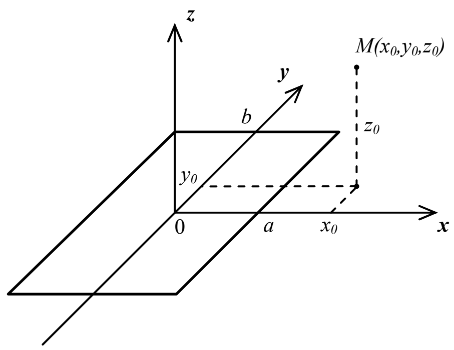

Fig. 3. **The position of the rectangular radiator in the Cartesian coordinate system**

The absolute value of the distribution of the complex acoustic pressure in the environment is calculated using expression [39]:

$$\left|\dot{P}_0\right| = \frac{\omega^2\rho}{2\pi}\sqrt{\mathrm{A}^2 + \mathrm{B}^2}, \tag{4}$$

where

$$\mathrm{A} = \int_{-a}^{+a}\int_{-b}^{+b}\dot{\xi}_0(x,y)\frac{\cos k\sqrt{(x-x_0)^2+(y-y_0)^2+z_0^2}}{\sqrt{(x-x_0)^2+(y-y_0)^2+z_0^2}}dxdy, \tag{5}$$

$$\mathrm{B} = \int_{-a}^{+a}\int_{-b}^{+b}\dot{\xi}_0(x,y)\frac{\sin k\sqrt{(x-x_0)^2+(y-y_0)^2+z_0^2}}{\sqrt{(x-x_0)^2+(y-y_0)^2+z_0^2}}dxdy. \tag{6}$$

When calculating the radiation pattern of the transducer shown in Fig. 1, the following expression is used [14-17]:

$$\xi_0(x,y)=\cos\left(\frac{3\pi}{2}\cdot\frac{x}{a}\right). \qquad (7)$$

Along the x-axis, the distribution of the amplitude of vibration is cosinusoidal. Along the y-axis, the distribution of the amplitude of vibration is constant. This is because the nodal lines of vibration are distributed parallel to this axis.

The distribution of acoustic pressure amplitudes in the environment is calculated using Eq. 4. These values, calculated in chosen planes and lines of the environment, are presented in Fig. 4 – 9. The calculation was made for normalized x and y coordinates with respect to the transversal dimensions a and b of the transducer.

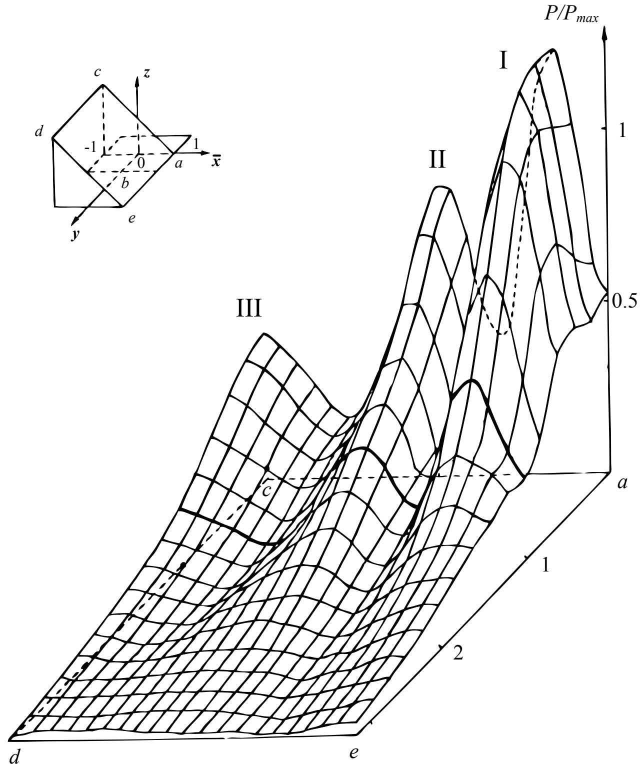

Fig. 4. **The distribution of acoustic pressure amplitudes (normalized values) in the plane *aedc* of environment when $a = b = l$**

In Fig. 4 the distribution of acoustic pressure amplitudes (normalized values) in the plane *aedc* of the environment, when $a = b = l$ is presented. As seen from Fig. 4, the distribution of acoustic pressure amplitudes has three different amplitude maximums of the acoustic pressure: I, II, III. The acoustic pressure along the y-axis reduces quickly. When $\bar{y}$ = 3, the acoustic pressure is practically zero.

Practical evaluation

In Fig. 5 the distribution of the acoustic pressure amplitude on the transducer's surface along the x-axis is presented.

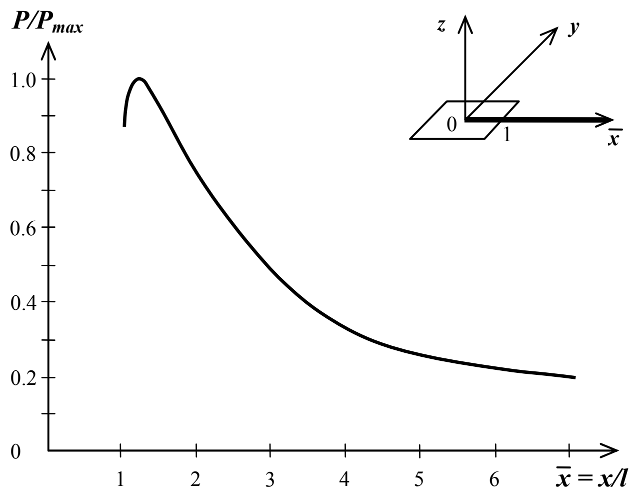

Fig. 5. **The distribution of acoustic pressure amplitude on the transducers surface along the x-axis**

With respect to the z-axis the distribution of the acoustic pressure P is symmetric.

At the distance of $\bar{x}$ = 10, the amplitude of the acoustic pressure approaches zero.

In Fig. 6 the distribution of the acoustic pressure amplitude on the line, which begins at zero coordinate and which is in a plane $z0x$, and which is equally tilted from the axes x and z at 45 degrees, is presented.

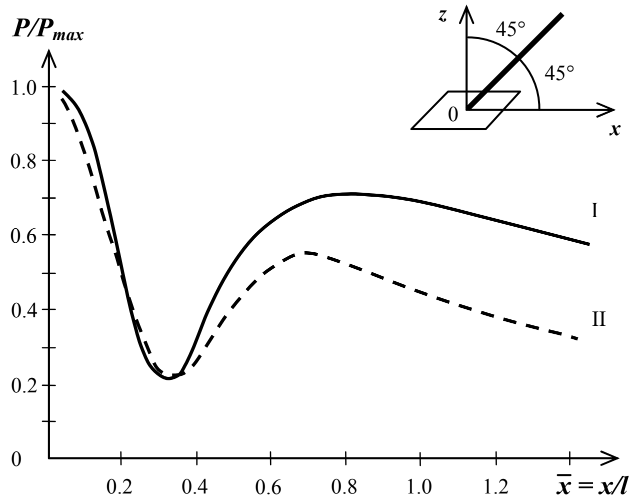

Fig. 6. **The distribution of the acoustic pressure amplitude on the line, which begins at zero coordinate and which is in a plane $z0x$, and which is equally tilted from the axes x and z at 45°: I – theoretical; II – experimental**

It can be seen from Fig. 6, that the near field of the transducer ends at approximately $\bar{x}$ = 0.8. For comparison, the near field of an oscillating piston is more than twice as long.

In Fig. 7 the distribution of the acoustic pressure amplitude on the line, which is parallel to x-axis, and which is in the plane $z0x$, and when $\bar{z}$ = 6, 8, 10 and $\bar{x}$ = 0 is presented.

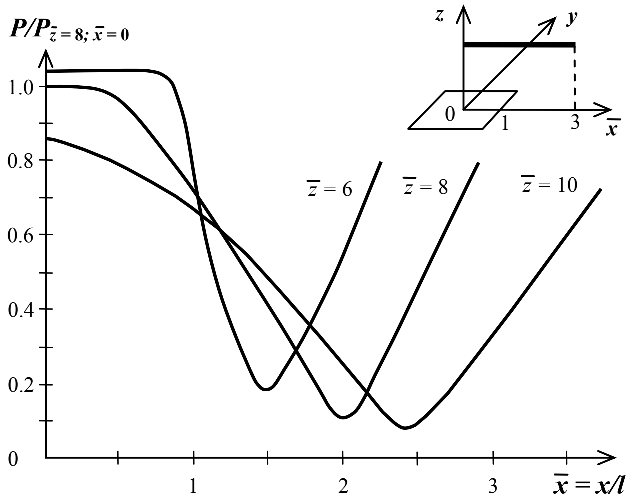

Fig. 7. **The distribution of the acoustic pressure amplitude along the line, which is parallel to *x*-axis, and which is in the plane *z*0*x***

The curves show that when $\bar{z}$ increases, the minimum of the acoustic pressure amplitude decreases, and the width of the radiation pattern increases.

In Fig. 8 the distribution of the acoustic pressure, calculated using Eq. 3, in a plane, tilted at 45° to *x*-axis, and which is beginning from *y*-axis, is presented.

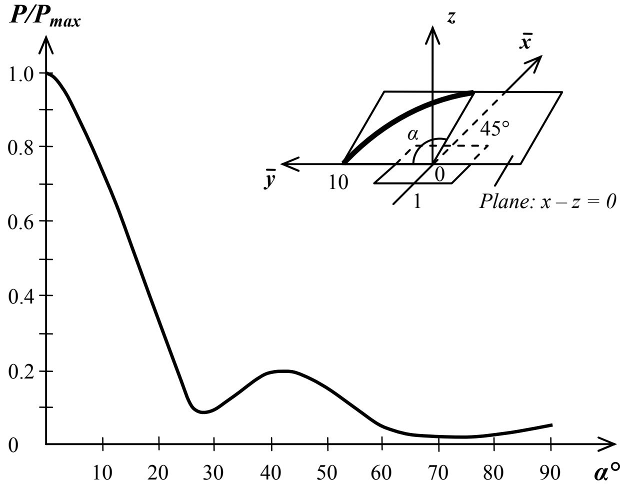

Fig. 8. **The distribution of the acoustic pressure amplitude in a plane, tilted at 45 degrees to *x*-axis, and which is beginning from *y*-axis, at the distance of $\bar{y}$ = 10 from 0 coordinate**

In Fig. 9, the distribution of acoustic pressure of the transducer in a plane *z*0*y,* at the distance of $\bar{y}$ = 10 from the zero coordinate, is presented.

From the calculated results we conclude that unidirectional radiation of the evaluated transducer in flexural vibration is achieved by a relatively small increase in the physical dimensions of the antenna [15, 16]. The schematic diagram of such antenna is presented in Fig. 10.

To achieve maximum radiation of the antenna, the vibrations of the transducers must be specially phased.

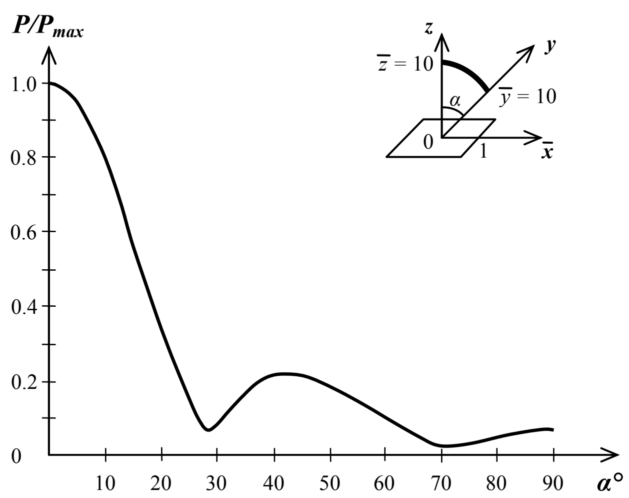

Fig. 9. **The distribution of acoustic pressure amplitude in a plane, *z*0*y*, at the distance of $\bar{y}$ = 10 from the zero coordinate**

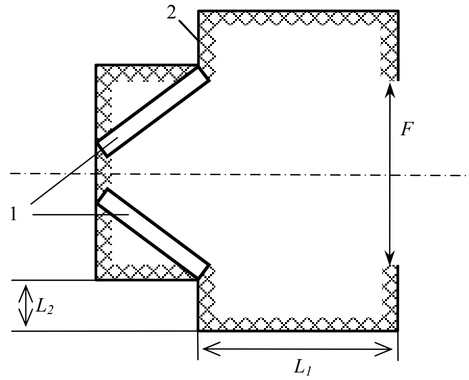

Fig.10. **Cross section of unidirectional acoustic antenna: 1 – rectangular bimorph piezoelectric transducers; 2 – absorber of acoustic radiation**

The papers [16, 17] show that the near acoustic field of a bimorph in flexural vibration is shorter than the field produced by an oscillating piston. It is possible to use this property to eliminate peripheral radiation by using sound-absorbing elements (Fig. 11).

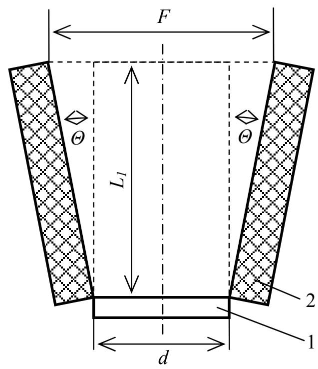

Fig. 11. **Cross section of unidirectional acoustic antenna: 1 – bimorph piezoelectric unidirectional transducer (or an array of such transducers like in Fig. 10); 2 – absorber of acoustic radiation**

The length L_1 of the absorber must meet this condition:

$$L_1 = (F/2) \cdot ctg\Theta , \quad (8)$$

where Θ is the angle between the maximum and the first minimum of radiation pattern; F is the aperture of the acoustic antenna.

In the antenna (Fig. 11) the absorber of acoustic radiation also serves as an element for matching acoustic impedances.

In Fig. 12, radiation patterns of the antenna (Fig. 10) are presented. The transducers were operating at the frequency 17 kHz. In this case, the distance L_1 was 130mm and the distance L_2 was 75mm. In Fig. 12a, the constructive elements of the reflector are made of metal. In Fig. 12b, the constructive elements of the reflector are made of styrofoam.

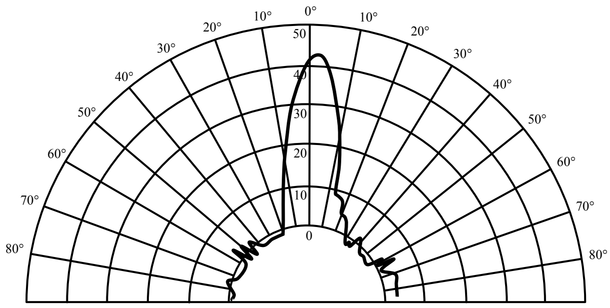

a

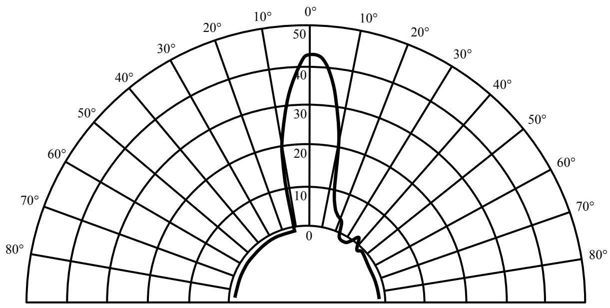

b

Fig.12. **Radiation patterns of the antenna (Fig. 10): a – metal reflector of acoustic waves; b – styrofoam absorber of acoustic waves**

As seen from these experimentally measured radiation patterns of the antenna, only the main leaf of radiation pattern is transmitted through the aperture to decrease the peripheral radiation. The peripheral radiation is damped by the constructive elements.

Conclusions

The near field of rectangular piezoelectric ceramic transducers with parallel nodal lines of vibration is significantly shorter in the direction of maximum radiation than of an oscillating piston.

The bimorph rectangular transducers with straight and parallel nodal lines of vibration can successfully be used when designing unidirectional acoustic antennas. The unidirectional radiation pattern of such antenna can be obtained by damping the peripheral radiation with constructive elements.

By using various passive constructive elements, physical dimensions of the acoustic antenna can be reduced to practically accepted sizes.

References

1. **Lin S.** Piezoelectric ceramic rectangular transducers in flexural vibration. IEEE Transactions on ultrasonics, ferroelectrics and frequency control. 2004. Vol. 51. No.7. P. 865-870.
2. **Lin S.** Study on the Langevin piezoelectric ceramic ultrasonic transducer of longitudinal-flexural composite vibrational mode. Yadian Yu Shengguang /Piezoelectrics and acoustooptics. 2005. Vol.27. No.6. P. 620-623.
3. **Shu-**Yu L. High power air-borne ultrasonic transducers. Acta physica Sinica (overseas Edition). 1999. 8 SUPPL. No.1. P. S38-S41.
4. **Xian X.**, Lin S. Study on the compound multifrequency ultrasonic transducer in flexural vibration. Ultrasonics. 2008. Vol. 48. No.3. P.202-208.
5. **Babic** M. A 200-kHz ultrasonic transducer coupled to the air with a radiating membrane. Ultrasonics, ferroelectrics and frequency control. IEEE Transactions. 1991. Vol.38. P.252 – 255.
6. **Yamane H., Kawamura M.** Sound sources with vibration plates in flexural modes and reflection plates for airborne ultrasonics. J. Acoust. Soc. Japan. 1976. Vol. 32. No.2. P.83-91.
7. **Bindal V. and Chandra M.** An improved piezoelektric ceramic transducer for ultrasonic applications in air. Archives of acoustics. 1982. Vol. 7. No.3-4. P. 281-286.
8. **Honda Y., Matsuhisa H. and Sato S.** Radiation efficiency of a baffled circular plate in flexural vibration. Journal of sound and vibration. 1983. Vol.88. No. 4. P. 437-446.
9. **Barone A., Gallego-Juarez J A.** Flexural vibrating free-edge plates with stepped thickness for generating high directional ultrasonic radiation. JASA. 1972. Vol.51. No.3. P.953-959.
10. **Germano C. P.** Flexure mode piezoelectric transducers. IEEE Transactions on audio and electroacoustics. 1971. Vol. AU-19. No.1. P.6-12.
11. **Домаркас В., Петраускас А.** Авт. Свид. СССР Nr.547975 (in Russian). B06B 1/06. 1977. Бюл. Nr. 7.
12. **Matsuzava K.** Sound sources for producing intense ultrasonic fields in small regions in air. In: Eighth International Congress on Acoustics. London. 1974. Vol.11. P.709.
13. **Kikuchi E.** Ultrasonic transducers (in Russian). Moscow: Mir. 1972. P.424.
14. **Petrauskas A.** Investigation and construction of measuring transducers for ultrasonic devices using flexural vibrations (in Russian). Ph. D. thesis. Kaunas. 1975. P. 147.
15. **Petrauskas A.** The optimization of directional characteristics for acustic antennas from piezoceramic rectangular bimorph transducers in flexural vibration. ISSN 1392 – 2114. Ultragarsas (Ultrasound). Kaunas: Technologija. 2007. Nr 1(62). P. 26-32.
16. **Petrauskas A.** Design and the radiation patterns of rectangular symmetric bimorph piezoelectric transducers in cosinusoidal flexural vibration. ISSN 1392 – 2114. Ultragarsas (Ultrasound). Kaunas: Technologija. 2009. Nr.1(64). P. 29-36.
17. **Petrauskas A.** A study of the design and the radiation patterns of rectangular bimorph acoustic transducers with thin piezoelectric ceramic plates. ISSN 1392 – 2114. Ultragarsas (Ultrasound). Kaunas: Technologija. 2008. Nr.4(63). P.57-65.
18. **Rayleigh L.** Theory of Sound (two volumes). New York: Dover Publications. 1987. Second edition. 1945 re-issue.
19. **Kaya O., Şahin A., Kaleci D.** Pressure field of rectangular transducers at finite amplitude in three dimensions. Ultrasound in Medicine & Biology. 2006.Vol. 32. Issue 2. P. 271-280.
20. **Minialga V., Petrauskas A.** Estimation of directivity patterns of two rectangular acoustic radiators oriented at various angles. ISSN 1392 – 2114 Ultragarsas (Ultrasound). Kaunas: Technologija. 1998. Nr.1(29). P. 20-23.
21. **Minialga V., Petrauskas A.** Testing and optimization of ultrasonic pulse locating antenna by laser vibrometer. Sixth International Conference on Vibrations Measurements by Laser Techniques: Advances and Applications, edited by Enrico Primo Tomasini. Proceedings of SPIE. 2004. Vol. 5503. P. 225-232.
22. **Ruzzene M.** Vibration and sound radiation of sandwich beams with honeycomb truss core. Journal of Sound and Vibration. 2004. 277 (4-5). P. 741-763. doi: 10.1016/j.jsv.2003.09.026.

23. **Sorokin S. V.** Vibrations of and sound radiation from sandwich plates in heavy fluid loading conditions Composite Structures. 2000. 48. (4). P.219-230. doi:10.1016/S0263-8223(99)00103-8.
24. **Li N.** Forced vibration analysis of the clamped orthotropic rectangular plate by the superposition method. Journal of Sound and Vibration, 1992. 158 (2). P. 307-316.
25. **Wu P., Kazys R., Stepinski T.** Analysis of the numerically implemented angular spectrum approach based on the evaluation of two-dimensional acoustic fields. Part I and II. J. Acoust. Soc. Am. 1996. Vol. 99. (3). P. 1339–1359.
26. **Farag N. H., Pan J.** Free and forced in-plane vibration of rectangular plates. Journal of the Acoustical Society of America. 1998. 103 (1). P. 408-413.
27. **Lin S.** Piezoelectric ceramic rectangular transducers in flexural vibration. IEEE Transactions on Ultrasonics, Ferroelectrics, and Frequency Control 2004. 51 (7). P. 865-870
28. **Lin S.** Study on the Langevin piezoelectric ceramic ultrasonic transducer of longitudinal-flexural composite vibrational mode. Yadian Yu Shengguang/Piezoelectrics and Acoustooptics. 2005. 27 (6). P. 620-623.
29. **Домаркас В., Мажонас А., Петраускас А.** Исследование характеристик направленности пьезопреобразователей изгибных колебаний (in Russian). ISSN 636-6367. Вильнюс: Минтис. Ультразвук (Ultrasound). 1983. Nr. 15. P. 48-51.
30. **Домаркас В., Мажонас А., Петраускас А**. Акустическое поле прямоугольных преобразователей изгибных колебаний с жестко закрепленными краями (in Russian). ISSN 0369-6367. Вильнюс: Минтис, Ультразвук (Ultrasound). 1986. Nr.18. P. 3-10.
31. **Мажонас А., Петраускас А.** Оптимизация характеристик направленности акустических антенн (in Russian). ISSN 0369-6367. Вильнюс: Минтис. Ультразвук (Ultrasound). 1984. No.16. P. 84-87.
32. **Danilov V. N., Ermolov I. N.** Estimation of the length of the near zone of a rectangular transducer. Russian Journal of Nondestructive Testing 2003. 39 (5). P. 333-338.
33. **Shuyu L.** Study on the radiation acoustic field of rectangular radiators in flexural vibration. Journal of Sound and Vibration. 2002. Nr. 254 (3). P. 469-479. doi:10.1006/jsvi.2001.4095.
34. **Sung C.-C., Jan J. T.** The response of and sound power radiated by a clamped rectangular plate. Journal of Sound and Vibration. 1997. 207 (3). P. 301-317.
35. **Mažeika L., Gresevičius M.** The fast technique for calculation of ultrasonic field of rectangular transducer. ISSN 1392-2114. Ultragarsas (Ultrasound). Kaunas: Technologija. 2008. Vol. 63. No. 4 P. 52-56.
36. **Gresevičius M., Jasiūnienė E., Mažeika L.** Comparison of simulations of ultrasonic fields of rectangular transducer. ISSN 1392-2114 Ultragarsas (Ultrasound). Kaunas: Technologija. 2008. Vol. 63. No.4. P. 22-27.
37. **Chen D., McGough R. J.** A 2D fast near-field method for calculating near-field pressures generated by apodized rectangular pistons J. Acoust. Soc. Am. 2008. Vol. 124. Issue 3. P. 1526-1537.
38. **Davy John L.** The directivity of the sound radiation from panels and openings. J. Acoust. Soc. Amer. 2009. Vol. 125. No. 6. P. 3795-3805
39. **Тюмин В. Н**. Введение в теорию излучения и рассеяния звука (in Russian). – Москва: Наука. 1976. P. 153-158.

A. Petrauskas

Antenų iš stačiakampių lankstymosi virpesių pjezoelektrinių keitiklių artimojo ir tolimojo lauko skaičiavimas

Reziumė

Nagrinėjamas akustinės antenos, sudarytos iš lanksčiai virpančių pjezokeraminių keitiklių, artimasis ir tolimasis sukuriamo slėgio laukas. Šis laukas apibrėžia antenos metrologines charakteristikas ir įgalina sukurti optimalias akustines antenas. Apžvelgiami praktiniai kryptingumo charakteristikų pagerinimo siekiant išvengti matavimams trukdančio periferinio spinduliavimo-priėmimo klausimai. Pateiktos rekomendacijos, kaip lanksčiai virpančius keitiklius panaudoti akustinėse antenose, kad galima būtų realizuoti vienkryptį spinduliavimą. Pateikti antenomis sukuriamo akustinio slėgio terpėje gauti skaičiavimo ir eksperimentiniai matavimų rezultatai ir pasiūlytos matavimams tinkamos pjezokeraminių keitiklių konstrukcijos.

Pateikta spaudai 2010 03 08

DOI: 10.5755/j01.u.65.1.17137